Available online at www.sciencedirect.com
SCIENCE DIRECT
Polymer 46 (2005) 11664–11672
polymer
www.elsevier.com/locate/polymer

Analysis of ductile and brittle failures from creep rupture testing of high-density polyethylene (HDPE) pipes

Rajendra K. Krishnaswamy *

Chevron Phillips Chemical Company, LP, Bldg 94-G, Bartlesville Technology Center, Bartlesville, OK 74004, USA

Received 30 March 2005; received in revised form 14 September 2005; accepted 16 September 2005
Available online 21 October 2005

Abstract

A comprehensive analysis of ductile and brittle failures from creep rupture testing of a wide spectrum of HDPE pipes was conducted. The analysis indicates that the ductile failure of such pipes is primarily driven by the yield stress of the polymer (or pipe). Examination of ductile failure data at multiple temperatures indicates a systematic improvement in performance with increasing temperature. It is proposed that testing at higher (above-ambient) temperatures leads to progressive relaxation of the residual stresses in the pipe; this causes the pipe to perform better as residual stresses are known to help accelerate the fracture process. Finally, our investigation indicates no correlation, whatsoever, between brittle failures in pressurized pipes and the PENT (Pennsylvania edge-notch tensile test; ASTM F1473) failure times. Therefore, one has to be extremely cautious in interpreting the true value of the PENT test when developing polymers and pipes for high-performance pressure pipe applications.

Keywords: Pipe; Polyethylene; Fracture

1. Background

The first plastic pipes were installed in the mid-1930s, with their usage increasing rapidly in the 1950s. Plastics have steadily replaced clay, copper, asbestos-cement, aluminum, iron and concrete pipes in various applications. Among the plastics employed in pipes, PVC accounts for about 75% while polyethylene is employed in about 20% of the plastic pipe applications [1,2]. High-density polyethylene (HDPE) pipes are used extensively for the transportation and distribution of natural gas, with over 80% of the new piping installations using HDPE. One striking example that highlights the strength of HDPE pipes can be found in the aftermath investigations of the Kobe (Japan) earthquake of 1995 during which the many fires and explosions from damaged gas pipelines caused considerable damage to life and property. However, there are no indications of HDPE pipe failure even under this extreme service condition. It was reported that the steel pipes failed and caused the aforementioned damage [3].

HDPE pipes used for gas transport are under pressure for the duration of their useful service. Often, fluctuations in pressure render the load to be dynamic. Therefore, it is important to establish the maximum load that such a pipe can withstand without deformation and damage over its expected lifetime (typically, many decades). It is highly impractical to predict the durability and the design stress of pipes using short-term tests such as the tensile or flexural tests. The design stress and the useful service lifetime of HDPE pipes are typically estimated by performing creep rupture tests at multiple temperatures. In this test, the pipe of interest is subjected to a certain hydrostatic pressure (expressed as hoop stress) and the failure time is recorded; failure is defined as a continuous loss of pressure (leakage) from within the pipe. Typically, a log–log plot of pipe hoop stress versus failure time is constructed and extrapolated to a desired lifetime. The corresponding hoop stress at the desired lifetime and temperature from the above-mentioned plot is used as the design stress (after the application of an appropriate safety factor) for the application of interest.

For polyethylene pipes, the plot of hoop stress versus failure time usually follows the schematic depicted in Fig. 1 [4]. In this figure, three distinct regions of failure are evident. Region-I, at higher imposed stresses, corresponds to ductile failure of the pipe and this is usually evident as a localized expansion (ballooning) of the pipe section under internal pressure. At lower stresses (region-II), the failure mode becomes brittle and is often characterized by the stable growth of a crack (slow crack growth or SCG) with little macroscopic plastic deformation. The transition from ductile to brittle failure

* Tel.: +1 918 661 9906; fax: +1 918 661 1709.
E-mail address: krishrk@cpchem.com

0032-3861/$ - see front matter © 2005 Elsevier Ltd. All rights reserved.
doi:10.1016/j.polymer.2005.09.084

mode in creep rupture testing is often referred to as the 'mechanical knee' or simply the 'knee'.

A majority of the field failures in pressure pipe applications are attributable to SCG. This has led to the development of many lab-scale tests, such as the Pennsylvania edge-notch tensile test (PENT; ASTM F1473) and the full notch creep test (FNCT; ISO 16770.3), to predict the resistance to SCG of various polyethylenes. The response of various polyethylenes to the dynamics of such lab-scale tests has been well documented [5–39]. Generally speaking, resistance to SCG improves with increasing molecular weight and with decreasing crystallinity (or density). Further, many investigators have pointed out that short chain branches (from suitable co-monomers) along the longest molecules of the molecular weight distribution is an especially effective manner to enhance resistance to SCG [16,19–29]. These observations point to the critical role exerted by the inter-lamellar tie-molecules on the SCG resistance of HDPE. The length of the co-monomer also appears to exert an influence on SCG, with HDPEs co-polymerized with 1-hexene displaying superior performance compared to those co-polymerized with 1-butene [25,30,31]. Some authors also suggest that crack growth can be accelerated along regions of low molar mass molecules segregated along the boundaries of crystalline superstructures [32–34].

When a given pipe is subject to hydrostatic loading for a considerably long period of time, failure is caused by chemical degradation of the polymer; this is referred to as region-III in Fig. 1. In region-III, the failure time is almost independent of applied stress. The transition from the brittle to the degradation failure mode is referred to as the 'chemical knee'.

Gas transport pipes are typically expected to last many decades. In order to predict the design stress and durability of such pressure pipes, accelerated testing is conducted at elevated temperatures. In other words, for a given pipe and hoop stress level, failure occurs at shorter times with increasing temperature. The location of the 'mechanical knee' shifts to lower hoop stress and shorter times as the test temperature is increased. The general procedure to estimate the design stress and durability of HDPE pipes requires creep rupture failure data spread uniformly over a 2-year timeframe at the end-use temperature (usually room temperature) and at two or three higher temperatures (typically in the 40–80 °C range). Subsequently, principles of time–temperature superposition are applied to the data; this allows one to reasonably extrapolate the failure data at room temperature to a few decades.

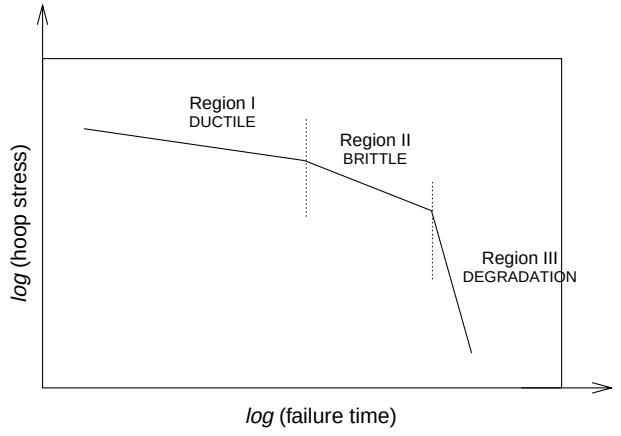

Fig. 1. Schematic of the typical hoop stress versus failure time plot for polyethylene pipes.

The design stress of a plastic pipe is often referred to as its long-term hydrostatic strength (LTHS) or the minimum required strength (MRS). LTHS, estimated using ASTM D2837 (USA standard), is the estimated tensile stress in the wall of a pipe in the circumferential orientation which, when applied continuously, will cause failure of the pipe at 100,000 h [40]. The MRS of a pipe, estimated using the ISO 9080 standard, is the functional equivalent of the LTHS (with a desired lifetime of 50 years) used internationally [41]. The LTHS and/or MRS of a pipe are used to certify gas pipes according to either ASTM D2513 [42] and/or ISO 4437 [43]. In other words, these values determine the maximum load that such pipes can bear during their utilization for the transportation of natural gas. It is, therefore, an important parameter not only for the pipe manufacturer and gas utilities, but also for the resin producer.

While HDPE has been successfully employed in pressure pipe applications for many decades now, a clear understanding of the relationships between molecular architecture and hydrostatic pressure performance is yet to emerge. Therefore, in this study, we intend to analyze pipe creep rupture data for many HDPEs of widely varying molecular architecture to develop a better understanding of the relationships between material properties and hydrostatic pressure performance as related to both ductile and brittle failures.

2. Experimental section

The HDPE resins investigated encompass a wide range of molecular architectures. Table 1 lists the polymer melt index, density and molecular weight characteristics. All of these polymers were produced using 1-hexene as the co-monomer. The data in Table 1 indicates a very wide spectrum of polymers employed in this investigation, with the weight average molecular weight (M_w) ranging from about 200 to

Table 1
Molecular characteristics of the polymers that were employed in this investigation

Polymer ID	Pellet density ASTM D1505 (g/cm^3)	Pellet HLMI ASTM D1238 (g/10 min)	M_w (kg/mol)	M_w/M_n
HDPE-A	0.950	2.4	460	51
HDPE-B	0.950	5.3	374	53
HDPE-C	0.949	2.2	500	59
HDPE-D	0.950	7.5	250	20
HDPE-E	0.952	5.7	227	14
HDPE-F	0.947	7.7	328	33
HDPE-G	0.943	13.0	200	25
HDPE-H	0.947	8.0	350	31

Table 2
Melt rheological characteristics, expressed in terms of the CY parameters, of the polymers that were employed in this investigation

Polymer ID	η_0 (Pa s)	τ_η (s)	a
HDPE-A	2.1×10^7	449.0	0.27
HDPE-B	9.8×10^6	160.0	0.27
HDPE-C	8.2×10^6	206.0	0.34
HDPE-D	2.6×10^5	1.4	0.31
HDPE-E	1.3×10^5	0.9	0.50
HDPE-F	1.6×10^7	169.0	0.16
HDPE-G	1.9×10^6	8.3	0.17
HDPE-H	1.1×10^7	96.7	0.16

500 kg/mol and the molecular weight distribution (M_w/M_n) ranging from about 10 to 60.

The melt rheology of the polymers was characterized by performing dynamic oscillatory measurements at 190 °C (using an ARES rheometer) and the resulting data ($|\eta^*|$ versus ω) were fitted to the Carreau–Yasuda (CY) model [44]:

$$|\eta^*(\omega)| = \eta_0[1 + (\tau_\eta\omega)^a]^{(n-1)/a} \quad (1)$$

where $|\eta^*(\omega)|$ is the scalar magnitude of the complex viscosity, η_0 is the zero-shear viscosity, ω is the angular frequency, τ_η is the characteristic viscous relaxation time, a is a parameter that is inversely related to the breadth of the transition from Newtonian to power-law behavior, and n fixes the final slope of the viscosity at high frequencies. The relevant CY parameters of all subject HDPEs are listed in Table 2. Amongst the polymers investigated, HDPE-A displays the highest η_0 (2.1×10^7 Pa s), while HDPE-E displays the lowest η_0 (1.3×10^5 Pa s). The melt relaxation time or τ_η is a function of both molecular weight and long chain branching (LCB) level in the polymer and may be used as an approximate indicator of melt elasticity. τ_η ranges between about 1 and 500 s for the subject polymers. Therefore, it is very clear that this investigation encompasses a very wide spectrum of molecular architectures.

The polymers listed in Tables 1 and 2 were all converted into pipe using fairly similar extrusion conditions. A 54 mm Davis Standard single screw extruder with a NRM two-stage screw was employed to produce the various pipes. An extrusion rate of approximately 68 kg/h was maintained during the production of all pipes, with the melt temperatures being in the 200–240 °C range (melt temperature depended on melt rheology). The outer diameter (OD) of all pipes was approximately 59 mm with a standard diameter ratio (SDR = OD/t) of about 11 (average wall thickness, t, of approximately 5.4 mm). Morphological characterization of the extruded pipes, as deduced by wide-angle X-ray diffraction, indicates close to random orientation of the lamellar crystals. All pipes contained approximately 2.5 wt% carbon black (for UV and weathering protection); the carbon black was introduced through dry-blending of the base polymer with a suitable carbon black master-batch prior to extrusion. All pipes were subjected to hydrostatic testing at room temperature (23 °C) and at elevated temperatures (60 and 80 °C) according to ASTM D1598-97 using various hoop stress levels at each test temperature.

The SCG resistance of the polymers was measured using the PENT test according to ASTM F1473. In some instances, the initial load was increased to 3.8 MPa to accelerate the fracture process. Tensile tests of the base polymers (compression molded by slow-cooling from the molten state) were performed using die-cut ASTM Type IV specimens using an Instron tensile tester. Tests at room temperature and at higher temperatures were performed in accordance with the ASTM D638-00 standard using a crosshead speed of 51 mm/min. The modulus, yield and break stress and strain were estimated from five measurements on each sample. A Perkin Elmer Diamond DSC, calibrated using indium and zinc standards, was used to characterize the melting behavior of the pipe samples. All of the non-isothermal scans were performed at 20 °C/min in a nitrogen atmosphere.

3. Results and discussion

In order to estimate the LTHS or the MRS of a given pipe, it is typical to gather creep rupture failure data (at multiple temperatures) covering a span of about 2 years. The procedure to estimate the LTHS of a pipe using ASTM standards is quite different compared to those used to estimate the MRS of a pipe using ISO standards. In our study, we will focus on the international (ISO 9080) protocol to estimate the MRS of HDPE pipes. Fig. 2 shows sample data at 20, 40 and 60 °C for a given HDPE pipe. First, at all temperatures, we see a systematic increase in the failure time with decreasing hoop stress. We also note acceleration of the fracture process at higher test temperatures. The transition from ductile to brittle failure (knee) is clearly evident at the higher test temperatures (40 and 60 °C), while it is absent at 20 °C (within the testing period). As expected, the location of this knee shifts to shorter times and lower stress levels at higher temperatures. Based on the location of the knee at 40 °C and at 60 °C, the location of the knee at 20 °C is predicted using time-temperature superposition principles.

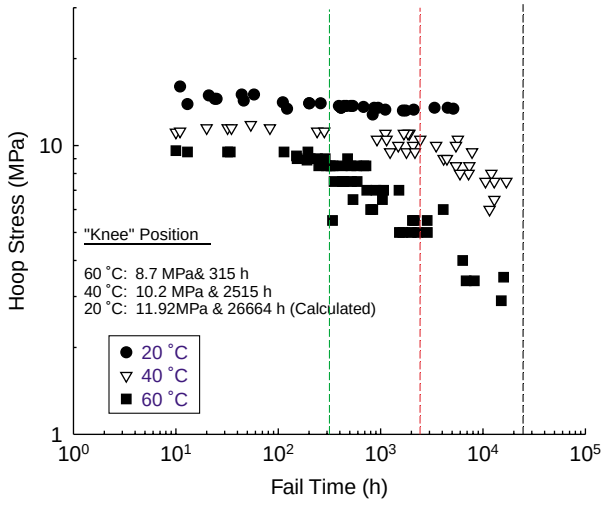

Fig. 2. Representative pipe hoop stress versus failure time data (at multiple temperatures) for a given HDPE.

3.1. Results: ductile failure

In this section, we will focus exclusively on the ductile failures of the subject HDPE pipes. In other words, we will focus only on data gathered at hoop stress levels high enough to produce ductile failure. In Fig. 3, a log–log plot of hoop stress versus failure time for the various HDPE pipes tested at 23 °C is shown. Only ductile failures were recorded at this temperature. In this figure, the failure data for each HDPE pipe was fit to the straight-line equation employed by the ISO 9080 protocol [41]:

$$\log t_{\text{fail}} = \left[A + \frac{B}{T}\right] + \left[C + \frac{D}{T}\right] \log \sigma_{\text{hoop}} \tag{2}$$

The straight lines in Fig. 3 are fits of the measured data (at least 15 data points for each pipe) to Eq. (2). A reasonable spread in the data is evident indicating a material dependence. In other words, for a given hoop stress, a wide range of failure times is evident for the different HDPE pipes. The inset in Fig. 3 shows the estimated failure time (from interpolation of existing data) for an imposed hoop stress of 11.0 MPa (at 23 °C) plotted as a function of the tensile yield stress of the polymer. A systematic linear dependence is evident on the semi-log plot suggesting an exponential increase in the ductile failure time (of pressurized HDPE pipes) with the tensile yield stress of the polymer (measured on compression-molded plaques). It is well established that the tensile yield stress of unoriented polyethylene is a strict function of its density or crystallinity [45–48]. Consequently, it is clear that the overall crystallinity is the primary contributor to the ductile failure of pressurized HDPE pipes.

It is important to note that the tensile yield stress of the pipe is different compared to the yield stress of the base polymer due to differences in thermal history and carbon black content. However, because we observe a systematic relationship between the yield stress of the polymer and that of the pipe (along the axial direction), we will only report the yield stress of the polymer in all of the subsequent analysis.

The ductile failure of pressurized pipes encompasses post-yield macroscopic stretching of the pipe section along the hoop direction until rupture [49]. Therefore, the applied hoop stress for the subject pipes was normalized with respect to the tensile yield stress of the base polymer:

$$\sigma^{N}_{\text{hoop}} = \frac{\sigma_{\text{hoop}}}{\sigma_{\text{yield}}} \tag{3}$$

In Fig. 4, the normalized hoop stress is plotted as a function of failure time for the various pipes. We note that the material dependence evident in Fig. 3 is strongly diminished, with data for the various pipes overlapping very strongly. This indicates that the ductile failure of pressurized HDPE pipes is a function of the applied hoop stress and the tensile yield stress of the polymer. In other words, the only material property of significance to the ductile failure of pressurized HDPE pipes is the tensile yield stress of the polymer.

While only ductile failures were evident for the pipes tested at 23 °C, it is typical for brittle failures to emerge within the nominal testing period at higher test temperatures (60

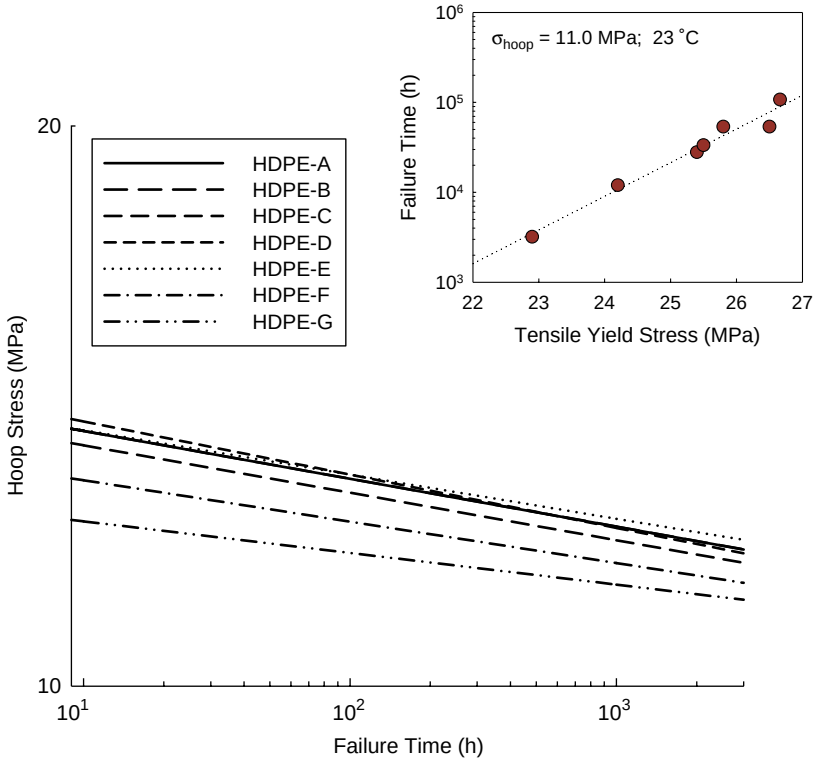

Fig. 3. Pipe hoop stress versus failure time data for all subject HDPE pipes at 23 °C. At least 15 failure data points were fitted to produce the best-fit lines shown in the plot. The inset shows failure time for an applied hoop stress of 11.0 MPa plotted as a function of the tensile yield stress of the polymer.

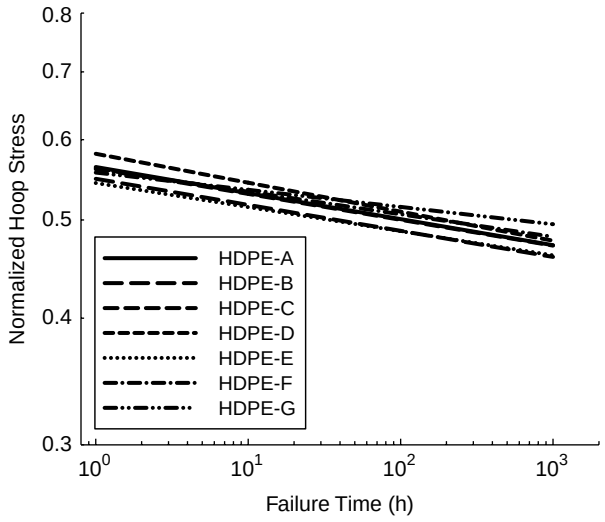

Fig. 4. Normalized pipe hoop stress ($\sigma_{hoop}/\sigma_{yield}$) versus failure time data for all subject HDPE pipes at 23 °C.

and 80 °C). The sample data in Fig. 2 shows the co-existence of ductile and brittle failure data at higher test temperatures. For the subject HDPE pipes, the ductile failure data at 60 °C and at 80 °C were fitted to Eq. (2). From the fit parameters for each pipe, the time to failure at a given hoop stress can be calculated. For ductile failures at 60 °C and at 80 °C, the time to failure displayed an exponential dependence on the yield stress of the polymer measured at the respective temperatures. In Fig. 5, the estimated ductile failure time (7.5 MPa hoop stress at 60 °C) for the various HDPE pipes is plotted as a function of the yield stress of the polymer measured at that temperature. This plot looks similar to the inset in Fig. 3. Consequently, at any test temperature well below the melting point of HDPE, it is clear that the failure time for ductile fracture of pressurized HDPE pipes depends primarily on the tensile yield stress of the polymer at that temperature. Therefore, our analysis of pipe creep rupture data indicate that the ductile failure of pressurized HDPE pipes depends primarily on the density of the polymer (or pipe) and is independent of molecular weight,

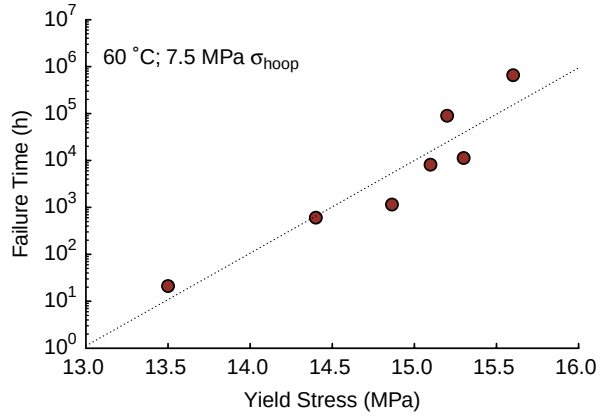

Fig. 5. Ductile failure time (60 °C; 7.5 MPa hoop stress) plotted as a function of the tensile yield stress of the polymer measured at 60 °C.

molecular weight distribution and branching content and distribution (at least for 1-hexene co-polymers).

Because of the wide spectrum of molecular architectures considered in our study, Fig. 4 can be considered (as a first approximation) to be a material-independent plot showing the ductile failure of pressurized HDPE pipes at 23 °C. It is then reasonable to combine data from all the different HDPEs and construct a single master-curve of ductile failures at 23 °C. Such a master-curve is shown in Fig. 6, where similar master-curves from analysis of ductile failure data at 60 and 80 °C are also included. It is surprising to note that these three normalized master-curves do not overlap. In fact, a systematic improvement in hydrostatic pressure performance with increasing temperature is clearly evident. In other words, for a given normalized hoop stress, the failure time for ductile fracture increases with increasing test temperature. While Fig. 6 only shows the material-independent master-curves, we have verified such a systematic improvement in performance for each of the HDPE pipes.

Fig. 7 shows the DSC melting traces of HDPE-A pipe; the melting endotherms for both the as-made pipe and an annealed (80 °C for 168 h) pipe are shown. The heat of fusion of the annealed pipe is only marginally higher than that of the as-made pipe. This increase in heat of fusion translates to about 1.5 wt% change in crystallinity. Besides the marginal increase in heat of fusion, annealing at 80 °C has caused some very thin lamellar crystals to melt and re-crystallize such that a slight shoulder in the primary melting endotherm is evident for the annealed pipe. Annealing experiments on the other pipes yielded similar (less than 2 wt%) changes in total crystallinity. A 1.5 wt% change in total crystallinity translates to an approximately 1.0–1.2 MPa increase in the tensile yield stress of polyethylene [46]. Therefore, while the increased crystallinity may account for a small improvement in the hydrostatic pressure performance of pipes tested at higher temperatures, it is difficult to explain the tremendous improvement in

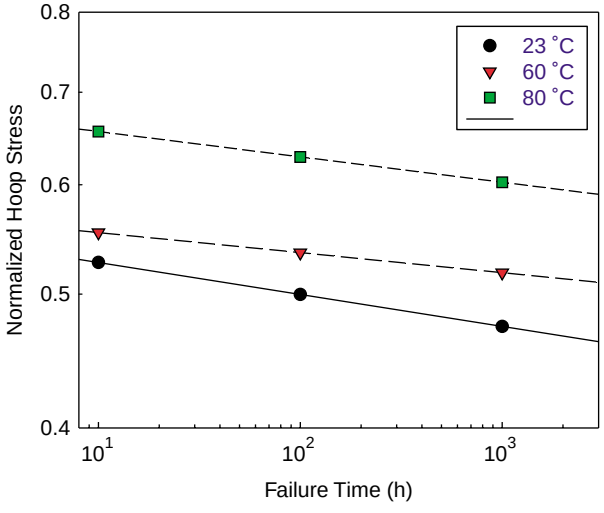

Fig. 6. Normalized pipe hoop stress ($\sigma_{hoop}/\sigma_{yield}$) versus failure time (material-independent) master-curves shown at the three test temperatures: 23, 60 and 80 °C.

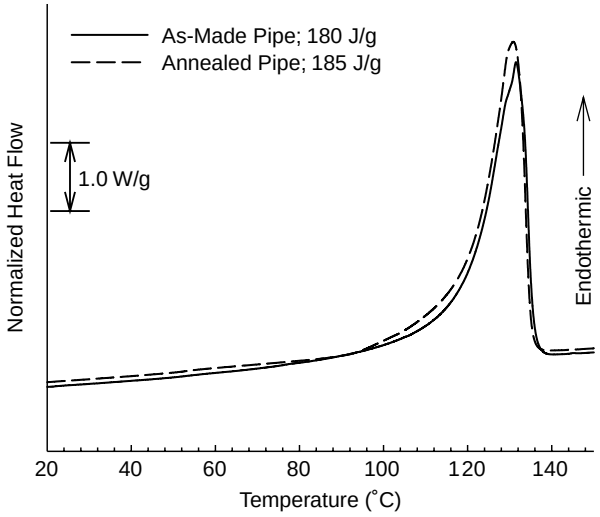

Fig. 7. Non-isothermal DSC sweeps (20 °C/min) of HDPE-A as-made and annealed pipes.

performance noted in Fig. 6. Consequently, we believe that other factors will have to be invoked to explain the observed improvement in ductile fracture resistance of pressurized HDPE pipes tested at above-ambient temperatures.

In a previous investigation [49], we had subjected a medium-density polyethylene (MDPE) pipe to hydrostatic pressure testing at a fixed hoop stress (such that ductile failure was induced) and temperature (23 °C). In this study, we had discovered that the failure times of the pipe was enhanced by approximately 300% when the pipes were simply annealed in an oven at 80 °C for 24 h prior to the creep rupture testing. This dramatic improvement in performance was attributed to relaxation of residual stresses within the pipe during the annealing step as the annealing treatment increased the crystallinity only marginally.

Residual stresses within a pipe (or any other extruded or molded part) are a consequence of a gradient in temperature during the fabrication process [50,51]. In pipe extrusion, the outside surface of the pipe is quenched (usually with a water spray) in the immediate vicinity of the die. The inner surface of the pipe, exposed to air, solidifies soon after the outer surface is set. This fixes the boundaries of the pipe. However, the inner core of the pipe wall solidifies several minutes after the pipe inner and outer surfaces have solidified. Therefore, as a consequence of the thermal gradient across the pipe wall, the crystallization (shrinkage) of the molecules within the core regions of the pipe wall produces residual stresses. It is reasonable to expect such residual stresses to accelerate the fracture process in tests such as creep rupture testing [50,51]. Some investigators [51–54] have tried to quantify the level of residual stresses in extruded HDPE pipes. These reports suggest that the residual stresses in extruded pipes are on the same order of magnitude as the design stress of the pipe. Specifically, residual stresses in the 2.0–5.0 MPa range appear to be fairly typical. These residual stresses act in tension along the inner wall of the pipe and in compression along the outer wall, with the absolute magnitude being greatest along the inner wall of the pipe [52]. Therefore, it is reasonable to expect these residual stresses to accelerate the fracture process of pressurized HDPE pipes [50]. In fact, one report [54] suggests that the ductile, brittle and low-temperature impact failure of pressurized HDPE pipes are adversely affected by the presence of residual stresses. This report further suggests that the extent of such adverse effects can be minimized by annealing at temperatures close to 80 °C.

It is well known that semi-crystalline polyethylene exhibits a glass–rubber transition well below ambient temperature [55–57]. Therefore, the mobility of the non-crystalline chain segments can be enhanced by simply increasing the temperatures to above-ambient levels. Further, closer examination of Fig. 7 reveals the onset of partial melting, which occurs at temperatures close to 60 °C for extruded HDPE pipes. Such partial melting and re-crystallization processes that occur at temperatures greater than 60 °C can serve to enhance the mobility of the non-crystalline chain segments considerably. Consequently, we argue that annealing at above-ambient temperatures will allow some of the residual stresses to relax. Such a reduction in residual stresses will lower the tensile stresses imposed along the inner wall of the pressurized pipe, causing it to perform better than expected. Therefore, the systematic improvement in pressure performance with increasing test temperature (Fig. 6) may be attributed primarily to a progressive relaxation of the residual stresses within the pipe and secondarily to a small increase in crystallinity.

The observations and analysis presented above clearly indicate that a simple time–temperature superposition of creep rupture data is an inaccurate means of estimating the design stress and durability of HDPE pipes. While the ASTM and ISO protocols embrace the concept of time–temperature superposition, appropriate safety factors are included in the calculations such that the error introduced by applying time–temperature superposition is perhaps accounted for. However, it is important to realize that, for HDPE pipes, microstructural changes and molecular re-arrangements that accommodate

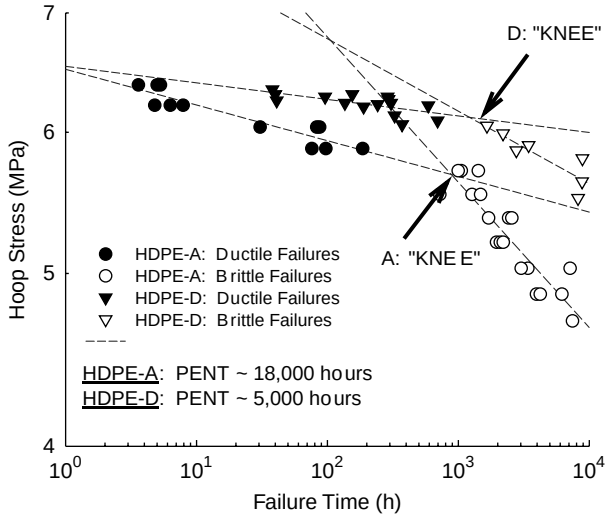

Fig. 8. Pipe hoop stress versus failure time data for HDPE-A and HDPE-D at 80 °C.

relaxation of residual stresses will occur at above-ambient temperatures; this is very likely to produce a better performing pipe.

3.2. Results: brittle failure

In HDPE pressure pipe applications, brittle failure is the most common mode of failure; it is characterized by the slow and steady growth of a crack that is initiated at a defect or stress concentration in the pipe. External factors such as rock impingement, squeeze-off and bending are known to accelerate the SCG fracture in gas transport pipes [58]. In creep rupture testing, the occurrence of early brittle failures can lower the effective design stress of the pipe and/or limit its durability. In Fig. 8, creep rupture data at 80 °C for HDPE-A and HDPE-D pipes are shown. For both pipes, the 'knee' or the transition from ductile failures at high stresses to brittle failures at low stresses is clearly evident. Specifically, the knee for HDPE-D occurs at much longer times compared to that of HDPE-A. This indicates that the HDPE-D pipe is generally more resistant to SCG failures compared to the HDPE-A pipe. However, the PENT failure times for the two polymers indicate otherwise with HDPE-A displaying much longer failure times (~18,000 h) compared to HDPE-D (~5000 h).

The PENT time to failure is often used to rank and grade various polyethylenes in terms of their SCG resistance. In Fig. 9, the location (time) of the knee at 80 °C for the subject HDPE pipes is plotted as a function of their PENT failure times. In this plot, the PENT failure times were measured using an initial load of 3.8 MPa (instead of 2.4 MPa) to accelerate the fracture process. It is clear from this figure that the PENT failure times are inadequate to predict the location of the knee in HDPE pipe creep rupture testing. Therefore, one has to be extremely cautious in relying on the PENT test to predict the performance of the ensuing pipe.

While we now recognize that the PENT measurement does not have much value in terms of predicting the occurrence of brittle failures in creep rupture testing, let us try to examine the dynamics of the PENT test in some more detail. During the PENT test, when a notched specimen is subject to a constant load, many stages of deformation are usually prevalent. However, only the ultimate failure time is recorded and reported. As a first approximation, the failure time can be said to be composed of three sequential deformation regimes; they are: (a) fracture initiation step; (b) slow crack growth; and (c) post-yield tensile stretching. The fracture initiation step is the time involved in the creation of the craze fibrils that initiate the fracture process. Once the craze fibrils have developed, crack propagation is accomplished through the rupture of the extended craze fibrils. Many investigations indicate that the fracture process in a creep test (like PENT) occurs in a step-wise fashion with the craze-zone formation and crack growth processes proceeding sequentially [11,35–37]. As the crack propagates, the ligament area decreases; this means, the ligament stress increases steadily during the test. It is then clear that the ligament stress will exceed the yield stress of the polymer at some point during the test such that notch blunting

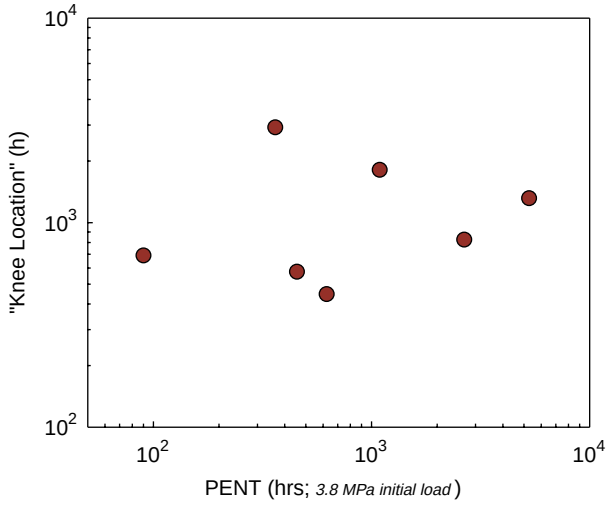

Fig. 9. Location of the 'knee' at 80 °C plotted as a function of the PENT failure times measured on the compression-molded specimens.

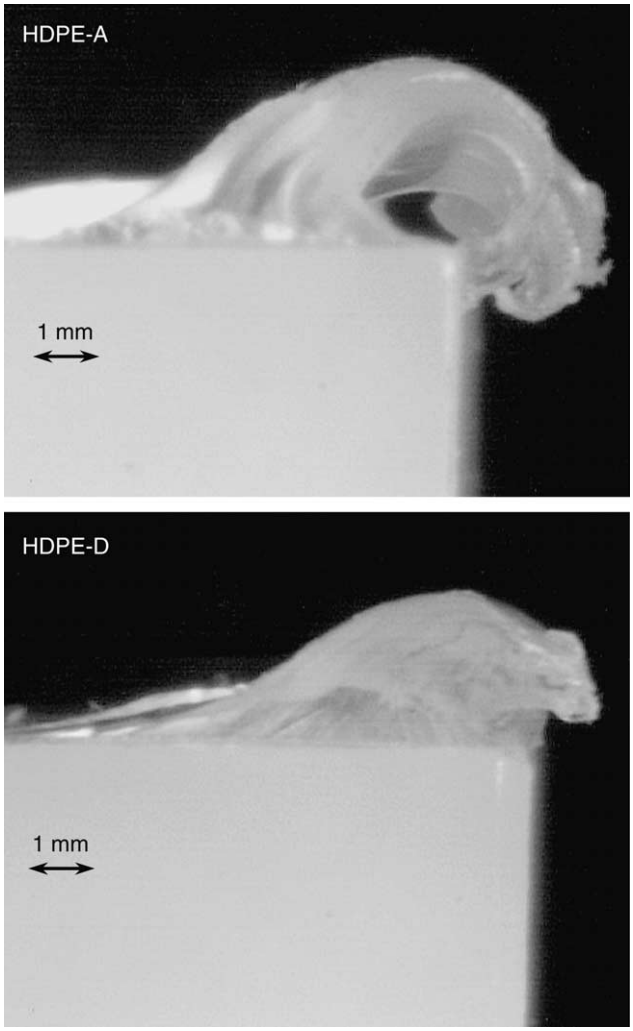

Fig. 10. Side-view pictures of failed PENT specimens for HDPE-A and HDPE-D showing the post-yield stretching that occurs at the end of the fracture process.

occurs and arrests the crack growth process. Subsequent deformation of the specimen occurs in a ductile fashion with ultimate failure occurring after the fibrils connecting the two halves of the specimen have been stretched completely.

Fig. 10 shows the side-views of failed PENT specimens for HDPE-A and HDPE-D. The edge opposite to the notched edge is shown in Fig. 10. These images clearly show macroscopic yielding for both polymers, with the extent of post-yield tensile stretching being considerably greater for HDPE-A. While it is clear that post-yield tensile stretching occurs towards the end of the PENT test, the relative contribution made by this deformation to the ultimate failure time is unclear.

It is perhaps reasonable to attribute the differences in the location of the knee (from creep rupture testing) for the various pipes to their varying fracture initiation resistance. However, the PENT failure times encompass the time-scale for fracture initiation, crack propagation and post-yield tensile stretching. Therefore, it is perhaps not surprising that there is no correlation between these two performance parameters. Many investigators have also followed the deformation process, in situ, during tests such as the PENT and FNCT using either microscopy or through extensiometers. These investigations have distinguished the relative times spent by various polymers in the different deformation regimes. Consequently, it is perhaps important that such instrumented creep tests be performed more routinely to develop a better correlation between lab-scale tests conducted on compression-molded specimens and creep rupture testing conducted on the ensuing pipes.

4. Conclusions

In this investigation, a very wide spectrum of HDPEs were chosen such that they differed considerably in their architectural and compositional make-up. These polymers were converted into pipe (constant dimensions) under fairly similar extrusion processing conditions. These pipes were subjected to extensive creep rupture testing (hydrostatic pressure testing) at multiple hoop stress levels and temperatures. Comprehensive analysis of the pipe creep rupture data indicates that the ductile failure of such pipes is primarily driven by the yield stress of the polymer. In other words, in creep rupture testing, the failure time is dependent only on the applied hoop stress and the yield stress of the polymer (or pipe) as long as the failure mode is ductile. At a given hoop stress and test temperature, the failure time for ductile fracture was observed to depend exponentially on the tensile yield stress of the polymer or the pipe. This means that the primary material property that contributes to the ductile failure of HDPE pipes is density or crystallinity; consequently, the ductile failure of HDPE pipes is independent of molecular weight, molecular weight distribution and branching (short and long) distribution.

Analysis of pipe creep rupture data at multiple temperatures indicates that a simple time–temperature superposition is not strictly applicable to predict the design stress and durability of pressure pipes. Normalization of ductile failure data at multiple temperatures indicates a systematic improvement in performance with increasing temperature in the range between 20 and 80 °C. Thermal characterization of the as-made and annealed (80 °C) pipes indicates marginal (less than 2 wt%) increase in crystallinity. While this small increase in crystallinity will contribute to longer failure times in the ductile failure mode, the level of performance improvement observed while testing at higher temperatures is considerably greater than can be accounted for by this change in crystallinity. Therefore, we propose that testing at higher (above-ambient) temperatures causes the residual stresses in the pipe to relax to some extent. This causes the pipe to perform better as residual stresses are known to help accelerate the fracture process. Consequently, one has to be careful about drawing conclusions from tests performed on compression molded specimens that are devoid of the microstructure and residual stresses that are typical of extruded pipes.

It is widely recognized that brittle fracture (through the initiation and subsequent crack propagation mechanism) at low stresses is the most common mode of failure for pressure pipes. Consequently, there has been considerable effort devoted to the duplication of such a fracture process in accelerated lab-scale tests. The development of PENT (ASTM F1473) is one outcome of such an endeavor. In our analysis of pipe creep rupture fracture, we find no correlation, whatsoever, between brittle failures in pressurized pipes and the PENT failure times. Therefore, one has to be extremely cautious in interpreting the true value of the PENT test when developing polymers and pipes for high-performance pressure pipe (PE100 and PE100+) applications.

References

[1] Mruk S. In: Mark HF, Bikales NM, Overberger CG, Menges G, Kroschwitz JI, editors. Pipe. Encyclopedia of polymer science and technology, vol. 11. New York: Wiley; 1988. p. 226.
[2] Stewart R. Plast Eng 2005;61:14.
[3] Nishimura H, Maeba H. Proceedings of the 10th international plastics pipes conference 1998 [Goteborg, Sweden].
[4] Gedde UW, Ifwarson M. Polym Eng Sci 1990;30:202.
[5] Brown N, Bhatacharya SK. J Mater Sci 1985;20:4553.
[6] Lu X, Brown N. Polymer 1987;28:1505.
[7] Wang X, Brown N. Polymer 1988;29:463.
[8] Lu X, Wang Z, Brown N. J Mater Sci 1988;23:643.
[9] Wang X, Brown N. Polymer 1989;30:1456.
[10] Lu X, Brown N. J Mater Sci 1990;25:411.
[11] Lu X, Qian R, Brown N. J Mater Sci 1991;26:917.
[12] Ward AL, Lu X, Brown N. Polym Eng Sci 1990;30:1175.
[13] Huang YL, Brown N. J Polym Sci, Polym Phys Ed 1990;28:2007.
[14] Huang YL, Brown N. J Polym Sci, Polym Phys Ed 1991;29:129.
[15] Huang YL, Brown N. Polymer 1992;33:2989.
[16] Lu X, Zhou Z, Brown N. Polym Eng Sci 1997;37:1896.
[17] Barry D, Delatycki O. J Polym Sci, Polym Phys Ed 1987;25:883.
[18] Barry D, Delatycki O. Polymer 1992;33:1261.
[19] Hubert L, David L, Sequela R, Vigier G, Degoulet C, Germain Y. Polymer 2001;42:8425.
[20] Hubert L, David L, Sequela R, Vigier G, Corfias-Zuccalli C, Germain Y. J Appl Polym Sci 2002;84:2308.
[21] Bohm LL, Enderle HF, Fleissner M. Adv Mater 1992;4:231.
[22] Ishikawa N, Shimizu T, Shimamura T, Goto Y, Omori K, Misaka N. Proceedings of the American gas association pipe symposium 1987.
[23] Scholten FL, Rijpkema HJM. Proceedings of plastics pipes VIII 1992.

[24] Clutton EQ, Rose LJ, Capaccio G. Proceedings of plastic pipes X 1998.
[25] Clutton EQ, Rose LJ, Capaccio G. Plast Rubber Compos Process Appl 1998;27:478.
[26] Lustiger A, Markham RL. Polymer 1983;24:1647.
[27] Lustiger A, Ishikawa N. J Polym Sci, Polym Phys Ed 1991;29:1047.
[28] Berthold J, Bohn LL, Enderle H-F, Gobel P, Luker H, Lecht R, et al. Plast Rubber Compos Process Appl 1996;25:368.
[29] Higuchi Y, Nishimura H, Tamamura H, Harada T. Proceedings of plastic pipes X 1998.
[30] Bubeck RA, Baker HM. Polymer 1982;23:1680.
[31] Wolfe AR. Proceedings of plastic pipes X 1998.
[32] Gedde UW, Jansson J-F. Polymer 1985;26:1469.
[33] Trankner T, Hedenqvist M, Gedde UW. Polym Eng Sci 1994;34:1581.
[34] Trankner T, Hedenqvist M, Gedde UW. Polym Eng Sci 1996;36:2069.
[35] Parsons M, Stepanov EV, Hiltner A, Baer E. J Mater Sci 1999;34:3315.
[36] Parsons M, Stepanov EV, Hiltner A, Baer E. J Mater Sci 2000;35:1857.
[37] Parsons M, Stepanov EV, Hiltner A, Baer E. J Mater Sci 2000;35:2659.
[38] Kadota K, Chudnovsky A. Polym Eng Sci 1992;32:1097.
[39] Chudnovsky A, Shulkin Y. Int J Fract 1999;97:83.
[40] ASTM D2837: Standard test method for obtaining hydrostatic design basis for thermoplastic pipe materials.
[41] ISO 9080: Plastics piping and ducting systems—determination of the long-term hydrostatic strength of thermoplastics materials in pipe form by extrapolation.
[42] ASTM D2513: Standard specification for thermoplastic gas pressure piping systems.
[43] ISO 4437: Buried polyethylene pipes for the supply of gaseous fuels—metric series—specifications.
[44] Rohlfing DC, Janzen J. In: Scheirs DC, Kaminsky J, editors. Metallocene-based polyolefins. New York: Wiley; 2000.
[45] Jordens K, Wilkes GL, Janzen J, Rohlfing DC, Welch MB. Polymer 2000; 41:7175.
[46] Janzen J, Register DF. In: Proceedings of the SPE ANTEC, vol. 2; 1996, 1996. p. 2190.
[47] Janzen J. Polym Eng Sci 1992;32:1242.
[48] Krishnaswamy RK, Yang Q, Fernandez-Ballester L, Kornfield JA. Submitted for publication.
[49] Krishnaswamy RK, Lamborn MJ. Adv Polym Technol 2005;46:266.
[50] Williams JG. Fracture Mechanics of Polymers. New York: Wiley; 1987.
[51] Williams JG, Hodgkinson JM. Polym Eng Sci 1981;21:822.
[52] Choollun VK, Wijeyesekara DC, Potter R. Proceedings of plastic pipes XII 2004.
[53] Janson L-E, Bergstrom G, Backman M, Blomster T. Proceedings of plastic pipes XII 2004.
[54] Vienne J, Vanspeybroeck Ph. Proceedings of plastic pipes XII 2004.
[55] McCrum NG, Read BE, Williams G. Anelastic and Dielectric Effects in Polymeric Solids. New York: Dover Publications; 1991 [©John Wiley and Sons (1967)].
[56] Boyd RH. Polymer 1985;26:323.
[57] Boyd RH. Polymer 1985;26:323.
[58] Palermo G. Proceedings of plastic pipes XII 2004.